

# Limits on the Molecular Gas Content of $z \sim 5$ LBGs

L. J. M. Davies<sup>1\*</sup>, M. N. Bremer<sup>1</sup>, E. R. Stanway<sup>1</sup>, M. Birkinshaw<sup>1</sup>, M. D. Lehnert<sup>2</sup>

<sup>1</sup>*Department of Physics, University of Bristol, H.H. Wills Physics Laboratory, Tyndall Avenue, Bristol, BS8 1TL, UK*

<sup>2</sup>*Laboratoire d'Etudes des Galaxies, Etoiles, Physique et Instrumentation GEPI, Observatoire de Paris, UMR8111 du CNRS, Meudon, 92195 France*

Accepted: July 21 2010

## ABSTRACT

We present limits on the molecular gas content of Lyman Break Galaxies (LBGs) at  $z \sim 5$  from observations targetting redshifted CO(1-0) and CO(2-1) line emission. We observed a single field containing eight spectroscopically-confirmed  $z \sim 5$  LBGs, seven of which are contained within a narrow ( $z=4.95 \pm 0.08$ ) redshift range and the eighth is at  $z = 5.2$ . No source was individually detected. Assuming the CO to H<sub>2</sub> conversion factor for vigorous starbursts, we place upper limits on the molecular gas content of individual  $z \sim 5$  LBGs of  $M(\text{H}_2) \lesssim 10^{10} M_{\odot}$ . From a stacking analysis combining all of the non-detections, the typical  $z \sim 5$  LBG has an H<sub>2</sub> mass limit comparable to their stellar mass,  $< 3.1 \times 10^9 M_{\odot}$ . This limit implies that, given the star formation rates of these systems (measured from their UV emission), star formation could be sustained for at most  $\sim 100$  Myr, similar to the typical ages of their stellar populations. The lack of a substantially larger reservoir of cold gas argues against the LBGs being UV luminous super starbursts embedded in much larger UV-dark systems and as a result increases the likelihood that at least those LBGs with multiple components are starbursts triggered by mergers. The sources responsible for reionization are expected to be starbursts similar to these systems, but with lower luminosities, masses and consequently with star formation timescales far shorter than the recombination timescale. If so, the ionized bubbles expected in the IGM during the reionization era will only infrequently have UV-luminous sources at their centres.

**Key words:** galaxies: high-redshift - galaxies: starburst - galaxies: star formation - radio lines: galaxies

## 1 INTRODUCTION

Detailed observations of the earliest galaxies are necessary if we are to form a complete picture of galaxy formation and evolution. While increasing numbers of spectroscopically-confirmed galaxies are being discovered at  $z \sim 5$  and above (within  $\sim 1$  Gyr of the Big Bang), almost all are discovered through rest-frame UV emission originating from strong ongoing star formation. Unfortunately, this tells us little about the (potentially dominant) UV-dark baryonic component of these galaxies and consequently limits our understanding of star formation in the high- $z$  universe.

Lyman-break Galaxies (LBGs) form a substantial part of current samples of  $z > 5$  galaxies (*e.g.* Vanzella et al. 2009; Douglas et al. 2009, 2010). They are identified *via* their UV continuum emission longward of 1216Å in the rest-frame, which arises from hot young stars formed in unobscured starburst regions. While *Spitzer*-based follow-up observations have made some progress in exploring and plac-

ing limits on their older underlying stellar populations (*e.g.* Eyles et al. 2007; Verma et al. 2007), we know little about their gas content, which is a crucial diagnostic of the duration of the ongoing starburst and of the nature of the LBGs themselves. The galaxies have unobscured star formation rates of a few  $\times 10 M_{\odot} \text{ yr}^{-1}$  arising from regions with a typical surface area of  $\sim 1 \text{ kpc}^2$ . The strong wind generated by such a starburst can potentially limit the available fuel for continuing star formation. Clearly, the amount of gas available to the ongoing starburst is key to an understanding of the nature of the burst and the future of star formation activity within the system. HST imaging of  $z \sim 5$  LBGs (*e.g.* Douglas et al. 2010; Conselice & Arnold 2009) shows that many systems have multiple UV components and extended, distorted morphologies on scales of a kpc or more. With the available optical and near-IR data, it is currently impossible to determine whether such structures imply that the LBGs originate in mergers, or are individual super starburst regions embedded in much larger UV-dark systems, as found in low redshift Lyman break analogues (Overzier et al. (2008), see Douglas et al. (2010) for a dis-

\* E-mail: Luke.Davies@bristol.ac.uk

cussion). If the latter scenario is correct, then one would expect considerably more cool and cold gas present in the immediate environment of the LBGs than is present in the stellar mass produced by the ongoing starbursts.

In this paper we probe the cool gas component of a sample of  $z \sim 5$  LBGs drawn from the ESO Remote Galaxy Survey (ERGS<sup>1</sup>, Douglas et al. 2007, 2009, 2010). Two of the ten 40 arcmin<sup>2</sup> ERGS pointings display a large over-density of spectroscopically-confirmed UV bright sources over narrow ( $\Delta z \sim 0.1$ ) redshift ranges. The first of these was the subject of a previous letter (Stanway et al. 2008) in which we discussed the identification of a UV-dark molecular line emitter at  $z \sim 5$ . Here, we target one field, J1054.4-1245, which contains many spectroscopically-confirmed LBGs in a two-arcminute diameter region. As in our previous work, we target the field using the Australia Telescope Compact Array (ATCA), but this time use the new Compact Array Broadband Backend (CABB) which probes a  $\Delta z \sim 0.6$  redshift range in a single exposure (at 38GHz). This is approximately 15 times broader than in our first work and easily encompasses the entire velocity range probed by the LBG over-density.

Throughout this paper, unless otherwise stated, all magnitudes are on the AB scale, and the cosmology used is  $H_0=70\text{kms}^{-1} \text{Mpc}^{-1}$ ,  $\Omega_\Lambda = 0.7$  and  $\Omega_M = 0.3$ .

## 2 OBSERVATIONS

Observations were carried out with the ATCA over two separate runs, one in May 2009 as part of project C1954 and another in March 2010 as part of project C2297. The primary goal of the project was to search for UV-dark molecular line emitters across our target field and the results of that study will be presented in a future paper. The array was in the compact H168 configuration, using both North-South and East-West baselines. We utilized the new CABB correlator with two intermediate frequency (IF) bands, each with 2GHz/2048 channel configurations. We targeted CO(2-1) and CO(1-0) transitions at the LBG over-density redshift. For CO(2-1) transitions we tuned the IF bands to 36.70 GHz and 38.72 GHz to allow a simultaneous survey range of  $4.81 \lesssim z \lesssim 5.44$ . We bin six adjacent 1 MHz channels to increase signal to noise, and we obtain a spectral resolution of  $\sim 47 \text{ km s}^{-1}$ . During the first run, observations were taken in six 8 hour periods between 2009 May 1 and 7. Three pointings were observed in order to target the maximum possible number of LBGs in the field. During the second run two additional pointings were observed in four 8 hour periods between 2010 March 21 and 23 (see figure 1). A nearby bright source, PKS1054-188, was observed every 15 minutes to determine the phase stability and the pointing accuracy was checked every hour. Primary flux calibration was carried out on the standard ATCA calibration source, PKS1934-638, each night. The half-power-beam-width (HPBW) of the ATCA at  $\sim 37 \text{ GHz}$  is  $74''$  and the restoring beam, for natural weighting and this configuration, is  $7.3'' \times 4.8''$ . For CO(1-0) transitions we tuned the IF bands to 19.12 GHz and 21.12 GHz giving redshift coverage of  $4.23 \lesssim z \lesssim 5.34$ . We

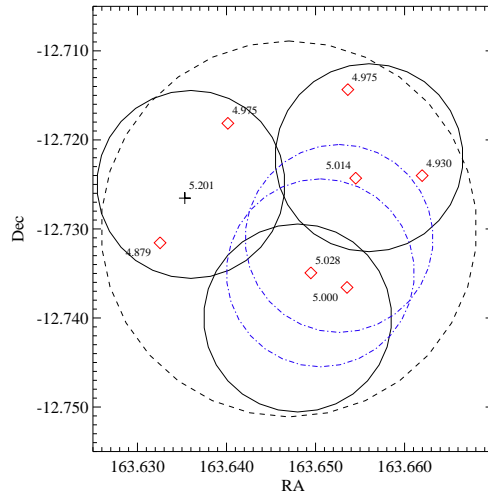


**Figure 1.** The spatial position of spectroscopically-confirmed LBGs in our target field. Red diamonds indicate LBGs in the narrowest redshift over-density, while the black cross shows the eighth LBG in this region at slightly higher redshift. Our ATCA pointings are indicated by the 7mm (solid circles for 2009 observations and dot-dashed blue circles for 2010 observations) and 12mm (dashed circle) half power beam widths. These encompass all eight LBGs.

observed a single pointing for two nights on 2009 May 8 to 9, encompassing all five  $\sim 37\text{GHz}$  pointings (see Figure 1). As before, we bin three adjacent 1 MHz channels to increase signal to noise which gives a resolution of  $\sim 47 \text{ km s}^{-1}$  (matching the velocity resolution of our high frequency data), use nearby source 1054-188 for secondary flux calibration and PKS1934-638 for primary flux calibration. The HPBW at  $\sim 20 \text{ GHz}$  is  $2.5'$  and the restoring beam is  $15.9'' \times 10.9''$ . At  $z \sim 5$  this corresponds to a beam size of  $> 50\text{kpc}$ .

We expect any detectable line emission from our sources to have velocity width  $\sim 150 \text{ km s}^{-1}$  (the only two known high redshift, non AGN, CO line-emitting galaxies at  $z \sim 5$  have line widths of  $\sim 160 \text{ km s}^{-1}$ , Coppin et al. (2010) and  $\sim 110 \text{ km s}^{-1}$ , Stanway et al. 2008) and we require detections to be statistically significant ( $> 2\sigma$ ) in each of 3 adjacent channels. Therefore by binning our data to 3MHz and 6MHz at the lower and higher frequency settings, a detection in three adjacent bins will correspond to a  $\sim 150 \text{ km s}^{-1}$ -wide line.

Total integration times were 16 hours at each frequency giving an rms noise of  $\sim 0.11 \text{ mJy/beam}$  at 19 GHz and  $\sim 0.17 \text{ mJy/beam}$  at 37GHz in each  $47 \text{ km s}^{-1}$  channel.

## 3 LIMITS ON LBG CO EMISSION

Our observations target eight spectroscopically-confirmed  $z \sim 5$  LBGs which are spatially distributed within the half power beam widths of individual pointings at both  $\sim 37\text{GHz}$  and  $\sim 19\text{GHz}$ . Seven lie in the 3-dimensional over-density ( $z \sim 4.95 \pm 0.08$ ) of LBGs in the larger ERGS field and the eighth is at slightly higher redshift ( $z \sim 5.2$ ). None of these galaxies show detectable line or continuum emission at either of the redshifted CO transitions targeted. For the

<sup>1</sup> ESO Program ID: 175.A-0706

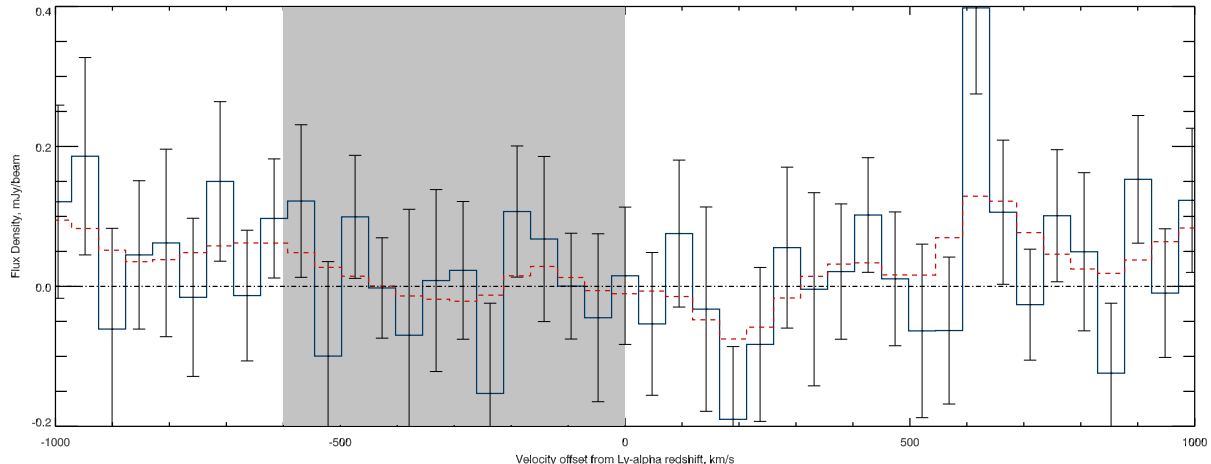


**Figure 2.** 1D spectrum of a typical LBG in our target region centered on the redshifted CO(2-1) line with redshifts assuming the Ly- $\alpha$  redshift. The blue solid line is the target spectrum (binned to 6MHz channels) with errors displaying the  $1\sigma$  rms error in a  $20'' \times 20''$  region around the LBG position. The red dashed line shows the target spectrum convolved with a  $150\text{ km s}^{-1}$  (FWHM) Gaussian. The shading highlights the region in which CO lines will be found given typical offsets between Ly- $\alpha$  and systematic redshifts. The most significant positive peak in the above spectrum at  $+650\text{ km s}^{-1}$  is still no more than  $2\sigma$  away from zero and consequently, given the number of independent bins displayed, is entirely consistent with noise.

line emission, each extracted 1-dimensional spectrum was examined for emission at the frequency expected for redshifted CO emission (using the redshift determined from either Ly $\alpha$  emission or the break at Ly $\alpha$  detected in optical spectroscopy Douglas et al. 2010). However, in a study of  $z \sim 3$  star forming galaxies, Steidel et al. (2010) show that the Ly $\alpha$  redshift can differ from the systematic redshift derived from interstellar absorption lines and other emission lines by up to  $\sim 600\text{ km s}^{-1}$ , with the Ly $\alpha$  redshift being systematically higher. Consequently, we additionally determined limits to any line flux at frequencies corresponding to velocity offsets of up to  $600\text{ km s}^{-1}$  shortward of the Ly $\alpha$ -derived value (see figure 2).

To search for CO line emission,  $47\text{ km s}^{-1}$ -wide slices of the data cube were extracted and the root-mean-square variation was ascertained in each for a region of  $\sim 20 \times 20$  arcsec box centred on the position of each LBG. Any real emission line is likely to be broader than  $50\text{ km s}^{-1}$  as noted above. Consequently, we define a detection as three consecutive  $47\text{ km s}^{-1}$  spectral bins at least  $2\sigma$  above zero flux in the region between 0 and  $600\text{ km s}^{-1}$  shortward of the Ly $\alpha$  redshift. Using these criteria, no individual source was detected. To determine a characteristic line-limit for each source, eleven values of the rms over three consecutive bins in the same 0 to  $600\text{ km s}^{-1}$  region were obtained. As the variation between these was small, we took the average value of these as characteristic of a given source. This results in a typical flux limit of  $< 60\text{ mJy km s}^{-1}$  for the CO(2-1) lines and  $\lesssim 40\text{ mJy km s}^{-1}$  for the CO(1-0) line. These correspond to luminosity limits in each line of typically  $1.1 \times 10^{10}\text{ K km s}^{-1}\text{ pc}^2$  at  $z \sim 4.95$  for CO(2-1) and  $2.6 \times 10^{10}\text{ K km s}^{-1}\text{ pc}^2$  for CO(1-0) (Solomon et al. 1997). Converting this to a limit on the molecular gas mass requires an appropriate conversion factor. In the absence of a directly measured value at the highest redshifts, we use the commonly-used conversion factor derived from lo-

cal strongly star forming galaxies (Solomon & Vanden Bout 2005) of  $M_{\text{gas}}/L'_{\text{CO}} = 0.8M_{\odot} (\text{K km s}^{-1}\text{ pc}^2)^{-1}$  given the strength of the starbursts in these LBGs. Assuming that the emitting medium is optically thick and thermalized, the line luminosity is independent of transition (*i.e.*  $L'_{\text{CO}}(2-1) = L'_{\text{CO}}(1-0)$ , Solomon & Vanden Bout (2005)). The typical CO(2-1) limit places a constraint on the gas mass of  $M_{\text{H}_2} \lesssim 8.9 \times 10^9 M_{\odot}$ . This is comparable to the stellar mass content of LBGs at this redshift (*e.g.* Verma et al. 2007; Stark et al. 2009). The constraint placed by the CO(1-0) line is a factor of two to four times higher depending upon the source.

Of course, if the line width is much narrower than we assumed, we may have missed emission using these criteria. However, we note that the above flux and luminosity limits are appropriate for a  $6\sigma$  non-detection of any emission confined to a single channel. In fact, no channel in the  $600\text{ km s}^{-1}$  range in any of the spectra deviates from zero by more than  $2.5\sigma$ , so the limit quoted above is robust.

In addition to determining limits on individual sources, we can derive deeper limits on the “typical”  $z \sim 5$  LBG by creating an average stack from the spectra of the eight individual sources, having shifted each spectrum to the same effective redshift. Concentrating on the CO(2-1) data and using the same criteria as for an individual spectrum, no line was detected in the averaged spectrum. The limits on the flux, line luminosity and  $\text{H}_2$  mass of a “typical” LBG are tightened to  $S_{\text{CO}}\Delta\nu \lesssim 17.5\text{ mJy km s}^{-1}$ ,  $L'_{\text{CO}(2-1)} < 3.9 \times 10^9\text{ K km s}^{-1}\text{ pc}^2$  and  $M_{\text{H}_2} \lesssim 3.1 \times 10^9 M_{\odot}$  at  $z = 4.95$  ( $2\sigma$ ).

However, this process is not completely straightforward as the true redshifts for the sources may not exactly match the Ly $\alpha$ -derived values, as noted above. The offsets between the Ly $\alpha$  and true values may vary by  $\sim 300\text{ km s}^{-1}$  between objects. Consequently, any combination of weak lines may be averaged in such a way that they are smeared out in

RA (Deg)	Dec (Deg)	Redshift	I (mag)	R-I (mag)	I-z (mag)	rms <sub>CO(2-1)</sub> <sup>1</sup> (mJy/beam)	L' <sub>CO(2-1)</sub> <sup>2</sup> (x 10 <sup>10</sup> K km s <sup>-1</sup> )	M <sub>H<sub>2</sub></sub> (CO(2-1)) <sup>3</sup> (x 10 <sup>10</sup> M <sub>⊙</sub> )
163.654	-12.7144	4.975±0.001	26.0±0.3	1.2±0.4	<-0.1	0.580	<1.28	<1.03
163.640	-12.7181	4.975±0.001	25.8±0.2	1.4±0.4	<-0.3	0.595	<1.31	<1.05
163.662	-12.7240	4.930±0.001	25.7±0.2	1.5±0.4	0.5±0.3	0.530	<1.17	<0.94
163.655	-12.7243	5.014±0.001	25.7±0.2	>2.3	0.6±0.3	0.409	<0.90	<0.72
163.635	-12.7265	5.201±0.001	26.1±0.3	>1.8	<0.0	0.583	<1.28	<1.02
163.633	-12.7316	4.879±0.001	25.8±0.2	1.3±0.4	<-0.3	0.584	<1.29	<1.03
163.649	-12.7349	5.028±0.001	26.2±0.3	>1.8	<0.1	0.334	<0.74	<0.59
163.654	-12.7366	5.000±0.001	26.1±0.3	1.3±0.5	<-0.0	0.348	<0.77	<0.61

**Table 1.** Properties of LBGs in target field (Positions given in J2000). **NOTES** - <sup>1</sup>Average of the total of the  $2\sigma$  rms errors in 3 adjacent bins (total in  $150\text{km s}^{-1}$  width) for all bins,  $600\text{km s}^{-1}$  blue-ward of the CO(2-1) line position if optical redshifts are correct. <sup>2</sup>Limit of CO luminosities derived from rms errors for an unresolved  $\sim 150\text{km s}^{-1}$  line (three channels at  $2\sigma$  rms limit). <sup>3</sup>Inferred gas mass derived from conversion factor for local infrared-luminous galaxies (Solomon & Vanden Bout 2005).

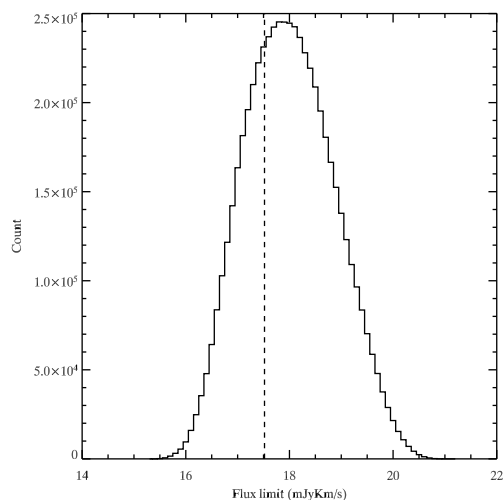


**Figure 3.** Histogram of the distribution of flux limits from 823543 possible iterations of stacking LBG spectra. Eight LBG spectra were combined varying the relative offset in redshift between seven of the spectra in six steps, +150, +100, +50, 0, -50, -100 and -150  $\text{km s}^{-1}$  relative to the eighth spectrum. The dashed line shows the flux limit for the eight spectra stacked at the optically-derived redshifts. The distribution of flux limits is Gaussian-distributed as expected given the noise characteristics of individual velocity channels.

frequency and do not reinforce each other to become a detection in the average spectrum. To explore this we made multiple average spectra, varying the relative offset in redshift between each spectrum in seven steps, +150, +100, +50, 0, -50, -100 and -150  $\text{km s}^{-1}$ , in total 7<sup>7</sup> or 823543 average spectra. We then take the ten flux limits in the -600 to  $0\text{km s}^{-1}$  region from each spectrum. The distribution of flux limits for these spectra are shown in figure 3. As can be seen, using the Ly $\alpha$  redshifts does not significantly underestimate the true value of the limit.

For completeness, we carried out the same procedure, but looking at features contained within a single bin as would be the case for extremely narrow lines. The highest flux in one of the -600 to  $0\text{km s}^{-1}$  bins in the average spectra was  $12.6\text{mJy km s}^{-1}$  (consistent with the noise characteristics given the 823543 different realisations), considerably

less than the above limit of  $S_{\text{CO}}\Delta\nu \lesssim 17.5\text{mJy km s}^{-1}$  and so we consider that limit to be robust even for a very narrow line.

## 4 DISCUSSION

Assuming that the conversion between CO luminosity and H<sub>2</sub> mass determined by Solomon & Vanden Bout (2005) is applicable (the intensity of the starbursts in these LBG indicates that it is), the non-detection of CO emission from these LBGs places interesting constraints on their nature. The similarity between the typical stellar masses of such systems as determined from multiband photometry of  $z \sim 5$  LBGs (Verma et al. 2007), and the limit to their typical H<sub>2</sub> mass (a few times larger) would indicate that the systems are observed about half way through the ongoing burst of star formation assuming that the current star formation rate is maintained and the conversions from gas to stars approaches  $\sim 100$  per cent efficiency. However, the efficiency with which gas is converted into stars is typically no more than ten per cent, and potentially only one or two per cent (Lehnert et al. 2009), thus suggesting that these sources are much more than halfway through their life cycle. This is unsurprising as timescales of  $\sim 10$  Myrs will be required to produce and sustain the observed UV continuum fluxes from a population of O and B stars. Dividing the limiting gas mass by the typical star formation rate from Verma et al. (2007) gives a timescale of  $\sim 100\text{Myr}$ , with the typical age of a stellar population determined by Verma et al. (2007) being a few tens of Myr. As this implicitly assumes an unrealistic complete transformation of gas into stars, even if the CO luminosity to H<sub>2</sub> conversion factor is higher than the Solomon & Vanden Bout value, this is a robust upper limit to the star formation timescale at this level of activity.

The apparent lack of a comparatively large reservoir of molecular gas in and around the UV-luminous system strongly argues against the LBGs being unobscured super starbursts embedded in much more massive and extended underlying systems. Any such system should contain sufficiently large amounts of enriched molecular gas to be detectable here. Consequently, it provides support for the alternative hypothesis of a merger origin for at least those systems with multiple spatially-distributed UV luminous components. If all  $z \sim 5$  LBGs are triggered by mergers with other galaxies, our lack of a single detection implies that few

involve comparatively massive systems with substantial obscured star formation or large amounts of processed molecular gas. Additionally, the most active phases of a merger occur when the gas has been consumed and is concentrated in the central regions of the systems. If LBGs are triggered by mergers, and given the need to build UV continuum fluxes through star formation, this may take substantial time. Therefore in this model LBGs may only be detectable (in the rest frame UV) towards the end of their starbursts. Observed luminous starburst galaxies at high- $z$  typically have short gas depletion times relative to their ages, similar to that seen in these sources. The lack of detectable 850 micron continuum flux in APEX/LABOCA observations of different but essentially similar LBGs (Stanway et al. 2010) gives further support to this model. As noted in Stanway et al. (2010) the conversions from continuum flux limits to star formation rates are currently ambiguous. However, the lack of detectable dust emission from these similar sources lends support to the idea that they do not have large reservoirs of cool and cold material, thus strengthening the idea that these sources are not embedded in more massive obscured systems.

There has been recent discussion (Papadopoulos & Pelupessy 2010; Gnedin & Kravtsov 2010) of whether there should be deviation away from the low-redshift Schmidt-Kennicutt (SK) relation (Schmidt 1959; Kennicutt 1998) at high redshift. Here we note that for unobscured star formation rates of a few tens of solar masses per year arising from regions of approximately  $\sim 1$  kpc (*e.g.* Verma et al. 2007; Bouwens et al. 2004; Bremer et al. 2004), a limit of  $M_{\text{H}_2} \lesssim 3.1 \times 10^9 M_{\odot}$  in the same area is consistent with the low-redshift SK relation. The synthesised ATCA beam at 38GHz probes an area of well over 100  $\text{kpc}^2$  centred on each LBG and so if there was an underlying larger UV-dark galaxy within which each LBG was embedded, any significant obscured star formation in that galaxy would lead to deviation from the nearby SK relation. As simulations imply that the relation gets steeper with redshift (more gas per unit star formation, *e.g.* Gnedin & Kravtsov 2010), the deviation from the SK relation would only increase if the nearby relation is inappropriate.

Given the comparatively brief elapsed time between the end of reionization and the redshift explored here, the limited gas reservoirs available for star formation in these systems and their relatively short star formation timescales have an important consequence for the reionization process. Reionization is likely to be dominated by as yet undetected faint, low mass UV-luminous starbursts (*e.g.* Lehnert & Bremer 2003; Salvaterra et al. 2010). As a consequence of their lower mass, these sources will have even shorter star formation lifetimes than the LBGs observed here. At all redshifts the recombination time for the IGM is longer than the Hubble time and hence also much longer than the UV-luminous lifetime of a low mass starburst. Consequently, most of the ionized bubbles expected to exist in the otherwise neutral IGM during reionization will only occasionally have UV-luminous sources at their centres, and most starbursts giving rise to the ionising flux will have long-since ceased to actively form stars and therefore have faded in the UV.

## ACKNOWLEDGEMENTS

LJMD and ERS gratefully acknowledge support from the UK Science and Technology Facilities council. Based on data from ATCA programs C1954 and C2297. The Australia Telescope Compact Array is part of the Australia Telescope which is funded by the Commonwealth of Australia for operation as a National Facility managed by CSIRO. The authors thank M. Voronkov and R. Ward for their assistance as Duty Astronomers at the ATCA.

## REFERENCES

- Bouwens R. J., Illingworth G. D., Blakeslee J. P., Broadhurst T. J., Franx M., 2004, *ApJ*, 611, L1  
 Bremer M. N., Lehnert M. D., Waddington I., Hardcastle M. J., Boyce P. J., Phillipps S., 2004, *MNRAS*, 347, L7  
 Conselice C. J., Arnold J., 2009, *MNRAS*, 397, 208  
 Coppin K., Chapman S., Smail I., Swinbank M., Walter F., Wardlow J., Weiss A., Alexander D. M., Brandt N., Dannerbauer H., De Breuck C., Dickinson M., Dunlop J., Edge A., Emonts B., Greve T., Huynh M., Ivison R., 2010, *ArXiv* 1004.4001  
 Douglas L. S., Bremer M. N., Lehnert M. D., Stanway E. R., 2010, *MNRAS* submitted  
 Douglas L. S., Bremer M. N., Stanway E. R., Lehnert M. D., 2007, *MNRAS*, 376, 1393  
 Douglas L. S., Bremer M. N., Stanway E. R., Lehnert M. D., Clowe D., 2009, *MNRAS*, 400, 561  
 Eyles L. P., Bunker A. J., Ellis R. S., Lacy M., Stanway E. R., Stark D. P., Chiu K., 2007, *MNRAS*, 374, 910  
 Gnedin N. Y., Kravtsov A. V., 2010, *ApJ*, 714, 287  
 Kennicutt Jr. R. C., 1998, *ApJ*, 498, 541  
 Lehnert M. D., Bremer M., 2003, *ApJ*, 593, 630  
 Lehnert M. D., Nesvadba N. P. H., Tiran L. L., Matteo P. D., van Driel W., Douglas L. S., Chemin L., Bournaud F., 2009, *ApJ*, 699, 1660  
 Overzier R. A., Heckman T. M., Kauffmann G., Seibert M., Rich R. M., Basu-Zych A., Lotz J., Aloisi A., Charlot S., Hoopes C., Martin D. C., Schiminovich D., Madore B., 2008, *ApJ*, 677, 37  
 Papadopoulos P. P., Pelupessy F. I., 2010, *ArXiv* 1005.3478  
 Salvaterra R., Ferrara A., Dayal P., 2010, *ArXiv* 1003.3873  
 Schmidt M., 1959, *ApJ*, 129, 243  
 Solomon P. M., Vanden Bout P. A., 2005, *ARA&A*, 43, 677  
 Solomon P. M., Downes D., Radford S. J. E., Barrett J. W., 1997, *ApJ*, 478, 144  
 Stanway E. R., Bremer M. N., Davies L. J. M., Birkinshaw M., Douglas L. S., Lehnert M. D., 2008, *ApJ*, 687, L1  
 Stanway E. R., Bremer M. N., Davies L. J. M., Lehnert M. D., 2010, *MNRAS* in press, (*arXiv*:1007.0440)  
 Stark D. P., Ellis R. S., Bunker A., Bundy K., Targett T., Benson A., Lacy M., 2009, *ApJ*, 697, 1493  
 Steidel C. C., Erb D. K., Shapley A. E., Pettini M., Reddy N. A., Bogosavljević M., Rudie G. C., Rakic O., 2010, *ApJ*, 717, 289  
 Vanzella E., Giavalisco M., Dickinson M., Cristiani S., Nonino M., Kuntschner H., Popesso P., Rosati P., Renzini A., Stern D., Cesarsky C., Ferguson H. C., Fosbury R. A. E., 2009, *ApJ*, 695, 1163  
 Verma A., Lehnert M. D., Förster Schreiber N. M., Bremer M. N., Douglas L., 2007, *MNRAS*, 377, 1024